International Journal of Microwave and Wireless Technologies

cambridge.org/mrf

Multi-pattern synthesis in fourth-dimensional antenna arrays using BGM-based quasi-Newton memetic optimization method

Avishek Chakraborty[1], Ravi Shankar Saxena[2], Anshoo Verma[3], Ashima Juyal[4], Sumit Gupta[5], Indrasen Singh[6], Gopi Ram[7] and Durbadal Mandal[8]

[1]Department of EECE, GST, GITAM University, Bengaluru, India; [2]Department of ECE, GMR Institute of Technology Rajam, Andhra Pradesh, India; [3]Department of CE, IES Institute of Technology and Management, IES University, Bhopal, India; [4]Uttaranchal Institute of Technology, Uttaranchal University, Dehradun, India; [5]Department of ECE, SR University, Warangal, Telangana, India; [6]School of Electronics Engineering, VIT Vellore, Tamil Nadu, India; [7]Department of ECE, NIT Warangal, Telangana, India and [8]Department of ECE, NIT Durgapur, West Bengal, India

Research Paper

Cite this article: Chakraborty A, Saxena RS, Verma A, Juyal A, Gupta S, Singh I, Ram G, Mandal D (2023). Multi-pattern synthesis in fourth-dimensional antenna arrays using BGM-based quasi-Newton memetic optimization method. *International Journal of Microwave and Wireless Technologies* 1–11. https://doi.org/10.1017/S1759078723000910

Received: 25 January 2023
Revised: 09 July 2023
Accepted: 11 July 2023

Keywords:
antenna arrays; memetic algorithm; monopulse radars; multifunctional radars; scanned beam patterns; shaped beam patterns; time-modulation

Corresponding author: Avishek Chakraborty; Email: avishekdreamz@gmail.com

Abstract

The advancement in wireless communication is fueling the growth of innovative antenna array designs toward cost-effective and performance-oriented solutions. This paper proposed unconventional methods to design antenna arrays for multi-pattern synthesis without using attenuators or phase shifters. A low-cost alternative is proposed with "Time-modulation"-based antenna array capable of electronic scanning and beam steering. Here, "Time" is utilized as a fourth-dimensional (4D) array parameter, and that is why "Time-modulated" arrays are also called as 4D antenna arrays. The idea is to control the high-speed switch attached with each antenna periodically to produce desirable current and phase tapering. This article expanded the "Time-modulation" concept to synthesize multiple radiation patterns like monopulse patterns, scanned beam patterns, shaped beam patterns, and cosecant-squared beam patterns for multifunctional radar systems. Suitable time schemes are developed to generate the narrowband sum–difference patterns useful for monopulse radars. Simultaneous scanned beam patterns are also proposed for narrowband communication. Furthermore, to address the wideband applications, shaped flat-top beam patterns and cosecant-squared beam patterns are also proposed. In this regard, 20- and 16-element "Time-modulated" linear array antennas are developed, and the parameters of the arrays are controlled by suitably designed objective functions with quasi-Newton method (QNM)-based memetic optimization method. For this purpose, first a well-known genetic algorithm is adopted to search the potential trust regions in the exploration stage and QNM is used for fine-tuning. Furthermore, the Broyden's good method-based direction-updating equation is used with QNM to improve the performance.

Introduction

Array antennas are the fundamental technologies of a modern communication system that has a broad range of applications in radar, remote sensing, satellite navigation, biomedical imaging, microwaves, and several other fields [1]. Since its introduction, antenna arrays have evolved substantially [2] and incorporated to multi-domain research prospect related to electromagnetics, electronics, computer science, control systems, etc. [3]. Phased arrays are the advancement over traditional antenna arrays usually considered for electronic beam scanning and beam steering [4]. Generally, the phased array antennas are equipped with transmit and receive modules that permit the independent control of amplitude and phase of the transmitted or received signals with the help of attenuators and phase shifters [4]. Cutting-edge communication system has thrusted stringent stipulation on phased arrays like multi-functionalities, reconfigurabilities, lesser weight, more compact, and reduced costs [4]. Further, the requirement of beamforming, beam scanning, and beam steering in advance communication systems has significantly increased the research concern in the domain of phased arrays. So, the exploration and exploitation of newer techniques for alternative solution is needed.

An unorthodox alternative to phased antennas has got the attention of antenna research community when Shanks et al. introduced the concept of fourth-dimension—"Time" to control the radiation patterns of antenna arrays [5]. Immediately after their path-breaking research, Shanks proposed a method for electronic scanning by utilizing the idea of

"Time-modulation" [6]. Although the "Time-modulated" array (TMA) was initially postulated for achieving ultra-low sidelobe radiation patterns [7], eventually they have become a popular choice for several other applications like electronic beam scanning [8], beam shaping [9], beam steering [10], and so on. TMAs may be classified as the "Time-domain" counterparts of traditional antenna arrays where a synchronized sequence is implemented with swiftly turning ON and OFF the RF switches, attached with each antenna element [11]. By adding and removing the elements from beamformer network (BFN), a desirable time-averaged radiation pattern can be generated [12]. The turn-ON period and switch-ON instants of each radiators can be controlled to obtain a sequence equivalent to the current and phase tapering in conventional arrays [12]. Hence, the need of costly phase shifters and erroneous attenuators may be eradicated, and the quantization error and insertion loss that occurred in traditional arrays may be avoided [13]. However, the added advantages of TMAs are also accompanied by the inherent drawback of infinite number of harmonic pattern generation due to the periodicity of the switches [14]. Harmonic radiations are generally considered unwanted because a major part of the dissipated power is transferred from the main beam to the sidebands [15]. The sideband radiation (SR) should be reduced to improve the total efficiency of the TMAs [16]. The primary research work in this field was focused only on sidelobe levels (SLLs) and SR reduction [17]. However, in due course, a new dimension has evolved with the notion of exploiting the unwanted SRs as an advantage. In this regard, TMAs for direction finding has been introduced [18]. The possibilities have been enhanced after Li et al. proposed a technique to steer the beam in some specific directions [19]. From then on, various research works have been reported with efficiently steered and scanned performances [20–25]. This paper exploited the notion further by proposing efficient multi-patterns such as sum–difference pattern for monopulse radars and scanned beam and shaped beam patterns for multifunctional radars (MFRs).

Monopulse-based searching and tracking radar require an array system that can produce a sum and a difference pattern simultaneously [26]. Tracking radar automatically keeps the main array beam aligned to the target object, producing a narrow and highly directive radiation pattern [27]. Monopulse arrays have been broadly employed in radar tracking systems to improve the poor speed and complicated BFNs experienced by a conical or sequential scanning [27]. The spatially independent and simultaneously generated harmonic beams can be used with appropriate switching sequence to deal with the drawbacks of compromised sum–difference patterns [28]. This article comes up with a suitable optimized switch scheme to produce the simultaneous monopulse pattern (sum–difference pattern) in a 20-element time-modulated linear array (TMLA). Further research on electronic beam scanning beneficial for the MFRs has been addressed by designing the suitable optimal time schemes [29]. Steering the consecutive harmonic patterns to prespecified angles and simultaneously lowering the SLLs is extremely beneficial for radars [30–32]. In this article, a 20-element TMLA is used to produce the scanned harmonic pattern at $\pm 30^{\circ}$ from the broadside. Furthermore, a shaped flat-top pattern is also targeted with a 16-element TMLA. To obtain the desired optimal radiation patterns, a memetic quasi-Newton optimization algorithm is employed. Here the limitations of traditional Newton method are eliminated by incorporating a Broyden's good method (BGM)-based direction-updating equation in the exploitation stage, along with the advantages of finding potential trust regions at the exploration stage using genetic algorithm (GA).

The work proposed in this article have manifold prospects briefly pointed out as follows:

- First of all, multiple patterns have been addressed by exploiting the concept of time-modulation.
- Second, for all the beam patterns, interference rejection is considered of the utmost importance.
- Third, to cancel the interference from unwanted sources, SLLs of all the patterns are minimized.
- Fourth, the unwanted higher-order harmonics apart from the first sideband are all suppressed.
- Fifth, the arrays are designed to cater the need of both the narrowband beam patterns using scanned beams and monopulse beams, as well as the wideband patterns using flat-top and cosecant beams.

The rest of the article is described as follows: The theoretical and mathematical insights of TMLA are presented in Section 2. The memetic algorithm used to optimize the control parameters is briefly discussed in Section 3. In Section 4, the outcomes of the proposed methods are analyzed, and a comparison and thorough discussion on future prospect is furnished. Finally, conclusive remarks are given in Section 5.

Theoretical background

Time-modulated linear arrays

A TMLA consists of N isotropic radiating antennas attached with same number of Single-Pole-Single-Through (SPST) Radio-Frequency (RF) switches, and it is controlled by a complex programmable logic device (CPLD), which is exhibited in Fig. 1. The array factor (AF) for the same may be given as [31]

$$\mathrm{AF}\,(\theta, t) = \mathrm{e}^{j(2\pi f_0)t} \sum_{n=1}^{N} I_n U_n\,(t)\,\mathrm{e}^{jk(n-1)d\,\cos\theta} \tag{1}$$

where I_n denotes the amplitude of the nth antenna, k is the constant of propagation, d represents the uniform spacing between antennas, θ is the angle of the impinging signal, f_0 is the operating frequency with T_0 as the period, and $U_n(t)$ is the time-switching function.

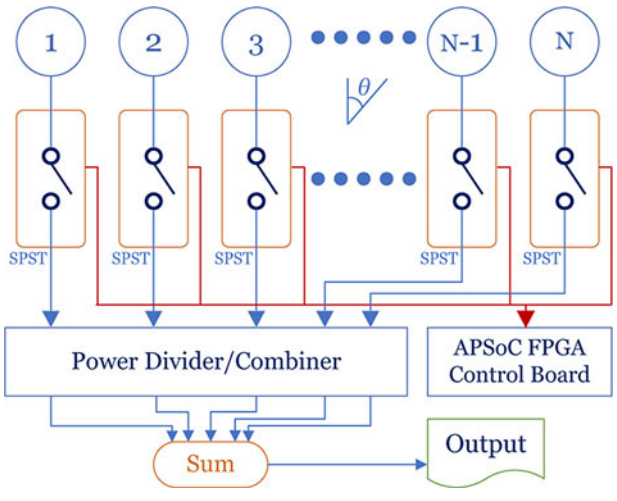

Figure 1. *N*-element array connected through switches and managed by a CPLD.

https://doi.org/10.1017/S1759078723000910 Published online by Cambridge University Press

Due to periodicity of switches, $U_n(t)$ can be given as [32]

$$U_n(t) = \sum_{m=-\infty}^{\infty} a_{mn} e^{jm(2\pi f_p)t} \tag{2}$$

The Fourier coefficient (a_{mn}) of nth element for mth frequency term, inherently generated because of time-modulation, can be presented as [33]

$$a_{mn} = \frac{1}{T_p} \int_0^{T_p} U_n(t)\, e^{-jm(2\pi f_p)t}\, dt \tag{3}$$

Hence, the AF of uniformly excited ($I_n = 1$) TMLA can be expressed as

$$\mathrm{AF}(\theta, t) = \sum_{m=-\infty}^{\infty} \sum_{n=1}^{N} a_{mn} \left\{ e^{jk(n-1)d\,\cos\theta} \right\} e^{j2\pi(f_0+mf_p)t} \tag{4}$$

The array pattern at mth harmonics may be simplified as [34]

$$\mathrm{AF}_m(\theta, t) = e^{j2\pi(f_0+mf_p)t} \sum_{n=1}^{N} a_{mn} e^{jk(n-1)d\,\cos\theta} \tag{5}$$

The main beam pattern can be represented with $m = 0$, and SR patterns are at the multitude of modulation frequencies (mf_p) where $m = \pm1, \pm2, \pm3, \ldots, \pm\infty$.

Time sequences for diverse applications of TMLAs may be designed, and to explore that, harmonic beam steering in TMLA is inscribed in the paper by suitably optimized shifted time sequences. The general ON–OFF time sequence for the nth antenna is given in Fig. 2(a), in which the radiator is turned on for the duration τ_n ($0 \le \tau_n \le T_p$). The pulse initiated at $\tau_n^1 = 0$ and terminated at τ_n^2 having a normalized ON-time duration $\{(\tau_n^2 - \tau_n^1)/T_p\}$. The switching function and the Fourier coefficient are given as [34]

$$U_n(t) = \begin{cases} 1, \tau_n^1 \le t \le \tau_n^2 \le T_p \text{ where } \tau_n^1 = 0 \\ 0, \text{otherwise} \end{cases} \tag{6}$$

$$a_{mn} = \frac{\tau_n}{T_p} \left\{ \mathrm{sinc}\left(m\pi f_p \tau_n\right) \right\} e^{-jm\pi f_p(\tau_n)} \tag{7}$$

The generalized shifted scheme of the nth antenna is given in Fig. 2(b), in which the ON-time duration of Fig. 2(a) is moved to τ_n^1 ($\tau_n^1 \neq 0$) and the nth antenna remains ON up to τ_n^2. The switching function and excitation coefficient for the shifted sequence can be given as

$$U_n(t) = \begin{cases} 1, 0 < \tau_n^1 \le t \le \tau_n^2 \le T_p \text{ where } \tau_n^1 \neq 0 \\ 0, \text{otherwise} \end{cases} \tag{8}$$

$$a_{mn} = \frac{(\tau_n^2 - \tau_n^1)}{T_p} \left[\mathrm{sinc}\left\{ m\pi f_p (\tau_n^2 - \tau_n^1) \right\} \right] e^{-jm\pi f_p(\tau_n^1 + \tau_n^2)} \tag{9}$$

For steering the first sideband patterns ($m = \pm1$) in prespecified direction (θ_0), the switching instants for each array element can be modified as [35]

$$\tau_n^1 = \left[\frac{(n-1)\, kd\, \cos\theta_0}{2\pi} - \frac{\tau_n}{2} \right] \mod 1 \tag{10}$$

The amount of radiated power for the fundamental pattern (P_0), the total power dissipated by harmonic patterns including the fundamental one (P_T), and the directivity can be given as [36]

$$P_0 = \int_{2\pi}^{0} \int_{\pi}^{0} |AF_0(\theta, \phi)|^2 \sin\theta \mathrm{d}\theta \mathrm{d}\phi \tag{11}$$

$$P_T = \sum_{\infty}^{m=-\infty} \int_{2\pi}^{0} \int_{\pi}^{0} |AF_m(\theta, \phi)|^2 \sin\theta \mathrm{d}\theta \mathrm{d}\phi \tag{12}$$

$$D = \frac{4\pi |AF_0(\theta_0, \phi_0)|^2}{\sum_{m=-\infty}^{\infty} \int_0^{2\pi} \int_0^{\pi} |AF_m(\theta, \phi)|^2 \sin\theta \mathrm{d}\theta \mathrm{d}\phi} \tag{13}$$

where the central beam pattern (at $m = 0$) points toward $\theta = \theta_0$, $\phi = \phi_0$ and $\mathrm{AF}_m(\theta, \phi)$ indicates the beam patterns generated at the mth-order harmonic frequencies ($m \neq 0$).

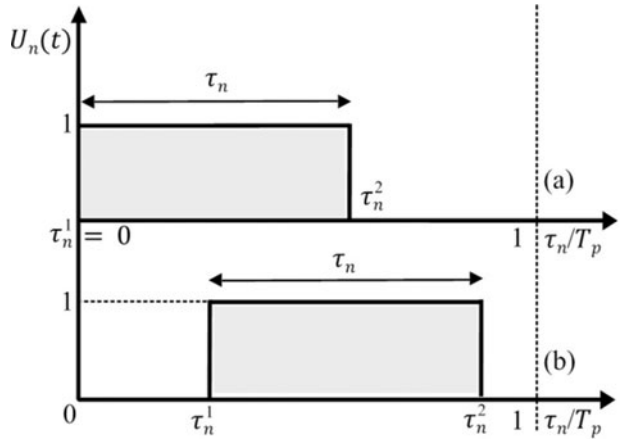

Figure 2. (a) Simple switching sequence and (b) shifted switching sequence for nth radiator in TMLA.

Objective functions

To manage the radiation characteristics of the central beam pattern and the steered SR patterns, the SLLs are lowered. The undesired higher sidebands are minimized. To obtain the coveted outcomes, an appropriate objective function (OF_1) is designed as

$$\mathrm{OF}_1 = (\mathrm{SLL}_0^{(i)})\big|_{f_0} + (\mathrm{SLL}_1^{(i)})\big|_{f_0 \pm f_p} + (\mathrm{SBL}_m^{(i)})\big|_{f_0 + mf_p} \tag{14}$$

where i denotes the current iteration, SLL_0 and SLL_1 represents the maximum SLLs at the fundamental (f_0) and first harmonic frequencies ($f_0 \pm f_p$), and SBL_m is the maximum level of sideband patterns ($f_0 + mf_p$ for $m = \pm2, \pm3, \ldots, \pm\infty$).

The exploitation of the harmonic radiations is concerned of highly directive radiation pattern generation for narrowband communication. On the other hand, the shaped pattern synthesis is aimed toward designing a flat-top pattern and the cosecant-squared pattern at the first sideband for specific wideband applications. The problems are cast into suitable OFs (OF_2 for flat-top and OF_3 for cosecant-squared patterns) as

$$\mathrm{OF}_2 = (\mathrm{SLL}_{\max}^{(i)})|_{f_0} + (\mathrm{Ripple}_{\max}^{(i)})|_{f_0+f_p} + \frac{\left(\beta_{\mathrm{Trans}}^{(i)}\right)}{90^\circ}|_{f_0+f_p} + (\mathrm{SBL}_m^{(i)})|_{f_0+mf_p} \tag{15}$$

$$\mathrm{OF}_3 = (\mathrm{SLL}_{\max}^{(i)})|_{f_0} + (\mathrm{Ripple}_{\max}^{(i)})|_{f_0+f_p} + \frac{\left(\beta_{\mathrm{Trans}}^{(i)}\right)}{90^\circ}|_{f_0+f_p} + (\beta_C^{(i)} - \beta_0)|_{f_0+f_p} \tag{16}$$

where $\mathrm{Ripple}_{\max}$ is the maximum ripple calculated at the first sideband, β_{Trans} is the transition width of the first sideband pattern,

https://doi.org/10.1017/S1759078723000910 Published online by Cambridge University Press

β_C is the calculated direction of the maximum power radiation, β_0 is the direction of maximum radiation in the desired plane. To minimize the OF_1, OF_2, and OF_3, a quasi-Newton method (QNM)-based memetic optimization technique is employed.

Quasi-Newton memetic optimization

Evolutionary optimization methods are population-based computational algorithms that help to unfold real-world technical issues by imitating the behavioral orientations of natural phenomenon [37]. Bioinspired computation methods have evolved as suitable candidates for solving electromagnetics problems [38]. Researchers have found these algorithms useful for synthesizing the radiation patterns of linear arrays [39, 40], circular arrays [41, 42], planar arrays [43, 44], concentric circular arrays [45, 46], hexagonal arrays [47], etc. Memetic algorithms are the population-based metaheuristics techniques, where the strengths of global search and the fine-tuning properties of local search techniques are combined [48]. GA is a familiar global search, stochastic optimization method based on natural selection and evolution [49]. GA has an excellent global search ability but requires a higher number of iterations for convergence [49]. On the other hand, deterministic QNM is the advanced version of the Newton method where a modified Hessian matrix is incorporated to minimize the computation cost and complexities of the Newton method. The hybridization of both can be regarded as a memetic computation method for solving nonlinear optimization problems [50]. In this paper, QNM-based memetic GA (QNM-GA) is employed.

The genetic algorithm

GA is a kind of probabilistic search method that utilizes the idea of natural selection and evolution. At each iteration, it preserves a population of individuals, also called as *Chromosomes*, coded from possible solutions (x_k) such as [50]:

$$x_k = x_{\min} + r_k\left(x_{\max} - x_{\min}\right) \tag{17}$$

where $x_{\min}$ and $x_{\max}$ are the lower and upper boundaries of the search space and r_k denotes some positive random values within the range of 0 and 1. *Chromosomes* are constructed over the binary range [0, 1] so that the *Chromosome* values can be uniquely mapped onto the decision variable domain. Each *Chromosome* is then evaluated by the fitness function, which is nothing but the representation of the optimization problem in hand. Based on that, elite strings are generated and *crossover* and *mutation* operations are done hereafter to generate the offsprings. In *crossover* operation, GA makes use of the following equation to produce two parent solutions x_s and x_t based on the *crossover rate* C_r as [50]:

$$x_{kj} = \begin{cases} x_{sj}, \text{if } C_r < r_{j0} \\ x_{tj}, \text{otherwise} \end{cases} \tag{18}$$

where r_{j0} is a random number within the range of 0 and 1. Then the *mutation* operation is done based on mutation rate parameter P_m as [50]:

$$x_{kj} = \begin{cases} x_{kj} + r_{j2}\left(x_{kj} - x_{mj}\right), \text{if } P_m < r_{j1} \\ x_{kj}, \text{otherwise} \end{cases} \tag{19}$$

where r_{j1} and r_{j2} are the random numbers within the range of 0 and 1. In this way, the genetic cycle updating continues iteratively until the completion of exploration stage for finding out the potential trust regions.

BGM-based QNM

Newton's method is an iterative method often used to solve the nonlinear equations due to its capability of rapid convergence from a sufficiently good starting position [51]. The limitation of Newton's method is the direct computation of Jacobian, which is computationally expensive [51]. In addition, the Newton's method is not suitable when the size is too large [52]. On the other hand, QNM is an updated version of Newton's method where the computation of Jacobian is skipped without affecting the locally super linear convergence characteristics [52]. QNM is based on the gradient method with double differentiation, implying better local search capability and faster convergence characteristic [53]. However, double differentials of antenna array are not possible as it is a simulation-based large-scale model [53]. Hence, a derivative-free QNM is adopted where BGM is used for updating the trust regions to get the best solutions for the problems in hand [53]. The brief overview of BGM-based QNM is discussed below:

Let us consider a set of nonlinear equations: $F(x) = 0, x\epsilon\, \Re^n$, where $F : \Re^n \rightarrow \Re^n$ is continuously differentiable and its Jacobian is denoted by (J_{x_k}). Here, x_k is the vector of variables such that $F(x_k)$ is the best cost value of the objective function at

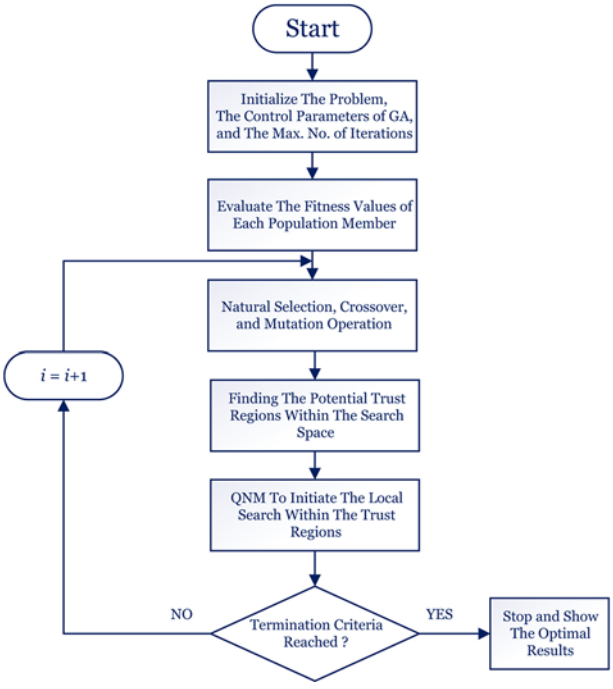

Figure 3. Flow chart of QNM-based memetic GA optimization.

Table 1. Control parameters of QNM-based memetic GA optimization

Control parameters	Values
Population size (x_k)	100
Number of iterations (i)	300
Mutation rate (P_m)	0.01
Crossover rate (C_r)	0.8
Selection probability	0.33
Step size (α_k)	0.0001
Random numbers (r_k, r_{j0}, r_{j1}, r_{j2})	[0,1]

https://doi.org/10.1017/S1759078723000910 Published online by Cambridge University Press

kth iteration. In a conventional Newton's method, calculation of Hessian matrix and the inverse of it is computationally expensive, especially when the dimensions are large. The Hessian of function $F: \Re^n \rightarrow \Re^n$ is the Jacobian of its gradient. In QNM, the Hessian is approximated by positive definite $n \times n$ symmetric matrix B_k that is updated iteratively such that the Hessian approximate (B_k) of Jacobian (J_{x_k}) must satisfy the quasi-Newton condition (secant equation) [51]:

$$B_{k+1}(x_{k+1} - x_k) = \nabla F(x_{k+1}) - \nabla F(x_k) \tag{20}$$

where the gradient vector is obtained from the first-order Taylor expansion of $\nabla F(x_{k+1})$ about $\nabla F(x_k)$ computed by finite difference method (FDM). The quasi-Newton condition of eq. 20 can be rewritten more succinctly by letting $\nabla F(x_{k+1}) - \nabla F(x_k) = y_k$ and $(x_{k+1} - x_k) = s_k$, so that we have [52]

$$B_{+1}s_k = y_k \tag{21}$$

For the derivative-free quasi-Newton equation, Broyden has further extended the updating equation, which is known as BGM. The update equation of BGM is as follows [53]:

$$B_{k+1} = B_k + \frac{(y_k - B_k s_k)\, s_k^T}{s_k^T s_k} \tag{22}$$

Finally, the derivative-free quasi-Newton equation for unconstrained optimization can be represented by incorporating the Broyden's method and direct line search method as [54]:

$$x_k^{\text{new}} = x_k + \alpha_k d_k \tag{23}$$

where α_k is the step size chosen to satisfy the Wolfe conditions, which is a set of inequalities used for line search in QNM. Here, $\boldsymbol{d}_k = -\mathbf{H}_k y_k$ denotes the Broyden-based direction, y_k is the gradient vector, and $\mathbf{H}_k$ is the Hessian that is approximated by BGM.

The gradient vector y_k in QNM is calculated using FDM, which is based on the idea of replacing derivatives with finite differences. It is not suitable for exploration as it may not be able to approximate the function derivatives [54]. Instead of that, GA can gradually converge to global optima and can be better fitted for the exploration stage to find out the potential trust regions in a multidimensional search space. That means step size will be smaller with the iterations going on. Then FDM can be used to exploit the trust regions in later evolution stage to produce the accurate results. The memetic method can be performed with a step-by-step process starting with the initialization of GA by setting the parameter values and population size for the concerned problem. After evaluating the fitness value of each population agent, crossover and mutation operation is executed iteratively to find the best possible trust regions. Then, QNM is applied to perform the local search within the potential trust regions for a finely tuned optimal solution. The whole process is repeated until the stopping criteria are reached [54]. The flow chart of the QNM-GA is shown in Fig. 3.

Numerical results

This section discusses several applications of TMLAs through distinct examples where QNM-GA method is adopted to obtain the optimized switching schemes for achieving the desired goals. The array is operating at 3 GHz (f_0) with 1 GHz of modulating frequency (f_p). The uniformly excited ($I_n = 1$) TMLA with a fixed inter-element spacing ($d = \lambda/2$) has these properties: −13.2 dB SLL,

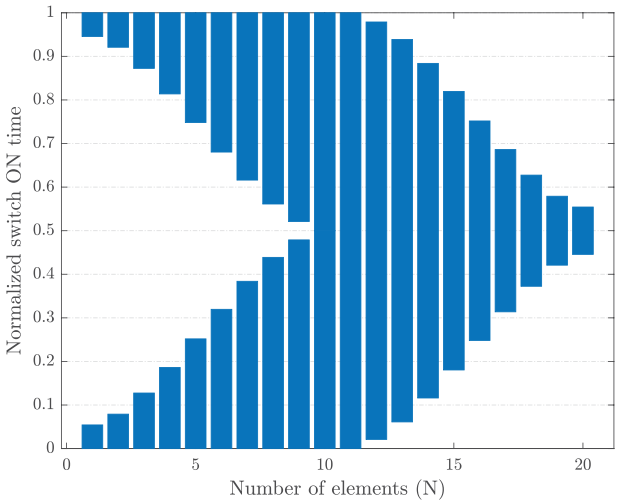

Figure 4. Switching sequence obtained with QNM-GA to get the sum–difference beam pattern in a 20-element TMLA for MTR.

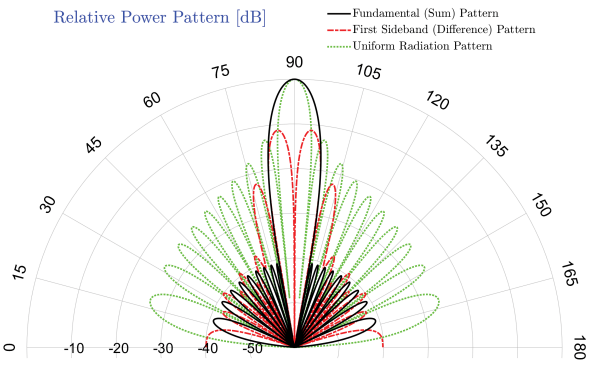

Figure 5. The corresponding sum pattern at central frequency and the squinted difference pattern at first harmonic obtained with QNM-GA-based optimal in and out-of-phase time sequence presented in Fig. 4.

6.48° half-power beamwidth (HPBW), 14.4° first-null beamwidth (FNBW), and a directivity of 12.04 dB. The numerical outcomes are simulated with MATLAB. The best-reported parameters of QNM-GA are used for the optimization process and also reported in Table 1 [54]. The proposed approach can also be considered with active elements using active element pattern method through pattern multiplication [55, 56]. But, for mathematical simplicity, only isotropic electromagnetic radiators are considered in this article. Further investigation is always possible by using different active elements with the proposed concept.

Monopulse scanned beam patterns

The simultaneous sum–difference beam for monopulse scanning is targeted using a 20-element TMLA. To achieve this target, an in-phase switching scheme for the first 10 radiators and an out-of-phase time scheme for the others with respect to array phase center is implemented. The notion is to design a switching scheme so that the OFF periods of the first 10 elements shall be the ON periods for the other 10. Hence, an in-phase and a reversed-phase tapering may be initiated. As a consequence, sum and difference beam with deep null toward the main beampattern (broadside direction)

https://doi.org/10.1017/S1759078723000910 Published online by Cambridge University Press

Table 2. Optimized ON-time period and starting times for multi-pattern synthesis

Patterns	Normalized ON-time period (ξ_n)					Normalized starting times (δ_n)				Spacing (λ_0)
Monopulse scanned beam patterns	0.1086	0.1581	0.2550	0.3723	0.5035	0.9457	0.9210	0.8725	0.8138	0.5
	0.6391	0.7677	0.8775	0.9577	1.0000	0.7483	0.6804	0.6161	0.5613	
	1.0000	0.9577	0.8775	0.7677	0.6391	0.5212	0	0	0.0212	
	0.5035	0.3723	0.2550	0.1581	0.1086	0.0613	0.1161	0.1804	0.2483	
						0.3138	0.3725	0.4209	0.4457	
Simultaneous scanned beam patterns	0.0938	0.0966	0.1385	0.1850	0.2338	0.9531	0.7017	0.4308	0.1575	0.5
	0.2815	0.3249	0.3609	0.3866	0.4000	0.8831	0.6093	0.3375	0.0695	
	0.4000	0.3866	0.3609	0.3249	0.2815	0.8067	0.5500	0.3000	0.0567	
	0.2338	0.1850	0.1385	0.0966	0.0938	0.8195	0.5875	0.3593	0.1331	
						0.9075	0.6808	0.4517	0.2031	
Shaped beam patterns	0.1225	0.1175	0.2313	0.3075	0.3025	0.8775	0	0.0780	0.1410	0.5
	0.3063	0.3625	0.4975	0.4975	0.3625	0.2040	0.2810	0.3640	0.3580	
	0.3063	0.3025	0.3075	0.2313	0.1175	0.3580	0.3640	0.2810	0.2040	
			0.1225			0.1410	0.0780	0	0.8775	
Cosecant-squared pattern	0.1500	0.1500	0.1500	0.2100	0.2600	0.6000	0.5250	0.5800	0.6200	0.5
	0.3500	0.4900	0.5500	0.5000	0.4700	0.6250	0.6200	0.6500	0.6400	
	0.4800	0.4700	0.4900	0.2000	0.1800	0.7100	0.7500	0.8000	0.8400	
	0.2100	0.1400	0.1500	0.1500	0.1400	0.9700	0.3500	0.8900	0.9400	
						0.1100	0.1000	0.1900	0.1800	

Table 3. Obtained simulation results for multi-pattern synthesis using QNM-GA

Patterns	SLL_0 (dB)	SLL_1 (dB)	$HPBW_0$ (°)	$HPBW_1$ (°)	$FNBW_0$ (°)	$FNBW_1$ (°)	P_U (%)	P_W (%)
Monopulse pattern	−40.89	−22.58	7.53	4.89	21.59	10.10	71.8152	28.1848
Steered pattern	−33.12	−23.53	6.84	7.56	18.36	18.36	73.5913	26.4087
Shaped pattern	−20.62	−20.32	33.12	7.92	49.20	20.88	76.7652	23.2348
Cosecant pattern	−20.17	−18.60	6.84	6.30	32.76	59.76	84.1802	15.8198

may be obtained at the same time. The QNM-GA-based switching scheme for the simultaneous monopulse scanned pattern is shown in Fig. 4, and the relative power patterns acquired by the switching sequence are given in Fig. 5. The desirable aim is to produce a sum pattern at the central frequency and a squint difference beam pattern at the first harmonics.

The suggested technique using a 20-element TMLA has achieved an ultra-low SLL_0 of −40.89 dB at fundamental frequency. The offset (SBL) in difference beam is calculated as −11.29 dB. The SLL_1 of the difference beam is obtained as −22.54 dB. The HPBW and FNBW of the relative power patterns attained at f_0 and $(f_0 \pm f_p)$ are 7.53° and 21.59°, and 4.89° and 10.1°, respectively. Out of total dissipated power, 71.8152% is utilized to produce the desired beams and 28.1848% is dissipated in higher sidebands. Thus, an efficient, controlled, and simultaneous monopulse scanned pattern is achieved with the suggested method beneficial for monopulse tracking radars (MTR). The optimized ON times and starting times are reported in Table 2. The results and the comparison with other published results are presented in Tables 3 and 4, respectively.

Simultaneous scanned beam patterns

The abilities of TMLA are further explored by exploiting the lower sideband patterns for scanning multiple beams. The undesired SR at harmonic frequencies is utilized by suitable time scheme to acquire the scanned beam patterns in some specific directions. The estimated direction of arrival observed for this problem is ±30° from the broadside.

The QNM-GA-based optimal time scheme for ±30° scanned beam patterns are given in Fig. 6, and the corresponding radiation patterns are presented in Fig. 7. The desired objective is to obtain the scanned beam patterns at ±30° from broadside. The first negative $(f_0 - f_p)$ and first positive $(f_0 + f_p)$ sideband beams are optimized to get the scanned harmonic patterns pointed at 60° (−30° shifted) and 120° (+30° shifted) while the fundamental beam at f_0 is pointing toward 90°. The central frequency beam has acquired a lowered SLL_0 of −33.28 dB. The SBL of first-order sideband beam ($|m| = 1$) is −1.45 dB. The SLL_1 of −23.58 dB is also acquired for the scanning patterns comparing with the highest level (i.e., the SBL). 73.5913% of total power is utilized in

https://doi.org/10.1017/S1759078723000910 Published online by Cambridge University Press

Table 4. Comparison of the proposed work for multiple pattern generation

Patterns	References	SLL_0 (dB)	SLL_1 (dB)	θ_0 (°)	θ_1	θ_{-1}
Monopulse pattern	Reference [9] (Case 1)	−23.7	−20.1	90	NR	NR
	Reference [9] (Case 2)	−40	NR	90	NR	NR
	Proposed (This work)	−40.89	−22.58	90	94.5	85.5
Steered pattern	Reference [33] (Case 1)	−11.1	−11.7	45	90°	NR
	Reference [33] (Case 2)	−19.2	−18.4	45	90°	NR
	Reference [57] (Case 1)	−17.13	NR	90	95.58	84.42
	Reference [57] (Case 2)	−16.3	NR	90	101.15	78.84
	Reference [57] (Case 3)	−16.8	NR	90	107.46	72.54
	Reference [35]	−21.7	−21.6	90	NR	60°
	Proposed (This work)	−33.28	−23.58	90	120°	60°

Note: θ_0, direction of the main beam; θ_1, scan angle for first positive harmonics; θ_{-1}, scan angle for first negative harmonics; and NR, not reported.

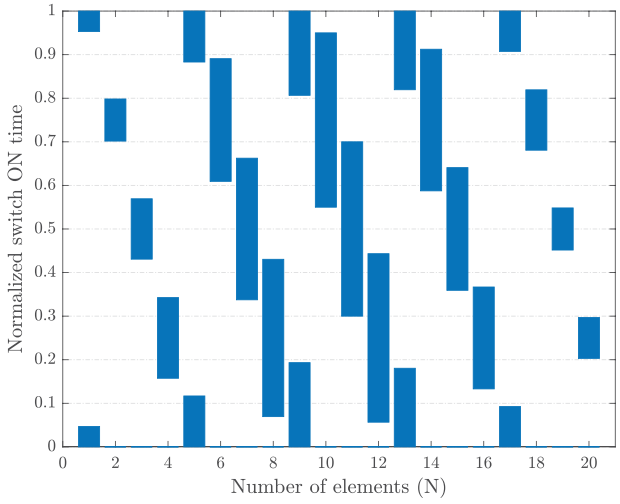

Figure 6. Switching sequence obtained with QNM-GA to generate scanned beam patterns in a 20-element TMLA for MFRs.

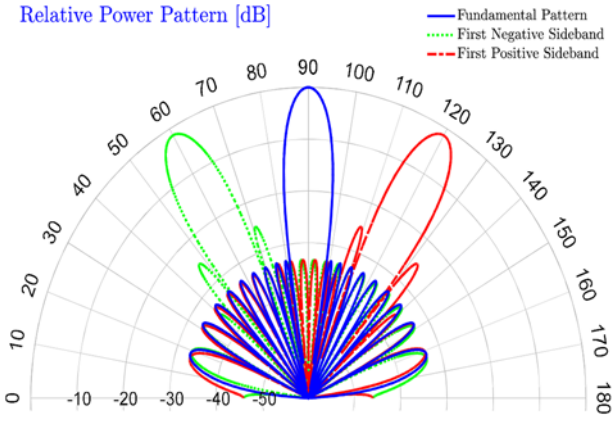

Figure 7. The corresponding scanned beam patterns at the first sideband frequencies ($|m| = 1$) with $\pm 30^\circ$ shifting from the broadside direction and the unaltered fundamental pattern, obtained with the QNM-GA-based time scheme presented in Fig. 6.

the desired beams and 26.4087% is dissipated in harmonics. The radiated power in the fundamental, first positive, and negative sideband beams are calculated as 31.2099%, 21.1907%, and 21.1907% of the total power. Thus, an alternative yet less costly solution for electronic scanning is proposed where the disadvantages of traditional phased arrays are eradicated. The optimized ON times and starting times are presented in Table 2. The results and the comparison with other published results are presented in Tables 3 and 4, respectively.

Shaped flat-top beam patterns

To obtain the shaped flat-top pattern, uniformly excited ($I_n = 1$) 16-element TMLA with equally spaced ($d = 0.5\lambda$) elements is optimized by QNM-GA, and the optimal switching scheme and the obtained radiation beam patterns are given in Figs. 8 and 9, respectively. The synthesized shaped pattern at the first sideband shows a wideband flat-top beam pattern of more than 30° width. A sharp transition of 7.56° is achieved with SLLs of −20.62 dB and −20.32 dB for the fundamental pattern and first sideband pattern, respectively. The power dissipated in flat-top shaped beam is measured as 21.2770% of total dissipated power, whereas the fundamental pattern used 34.2112% of the radiated power. 76.7652% of radiated power is utilized for the desired synthesized patterns, and 23.2348% of the power is dissipated in higher-order harmonics. The optimized ON times and starting times are presented in Table 2, and the results are shown in Table 3.

Cosecant-squared beam patterns

To obtain the cosecant-squared pattern, uniformly excited ($I_n = 1$) 20-element TMLA with equally spaced ($d = 0.5\lambda$) elements is optimized by QNM-GA, and the optimal switching scheme and the obtained radiation beam patterns are given in Figs. 10 and 11, respectively. The synthesized cosecant-squared beam pattern at the first sideband as well as the fundamental pattern has also been considered for SLL reduction. The SLLs of −20.17 dB and −18.6 dB is achieved for the fundamental pattern and cosecant-shaped first sideband pattern, respectively. The power dissipated in desired patterns is measured as 84.18% of total dissipated power, whereas the remaining 15.82% is wasted in higher sidebands. The optimized ON times and starting times are presented in Table 2, and the results are shown in Table 3.

https://doi.org/10.1017/S1759078723000910 Published online by Cambridge University Press

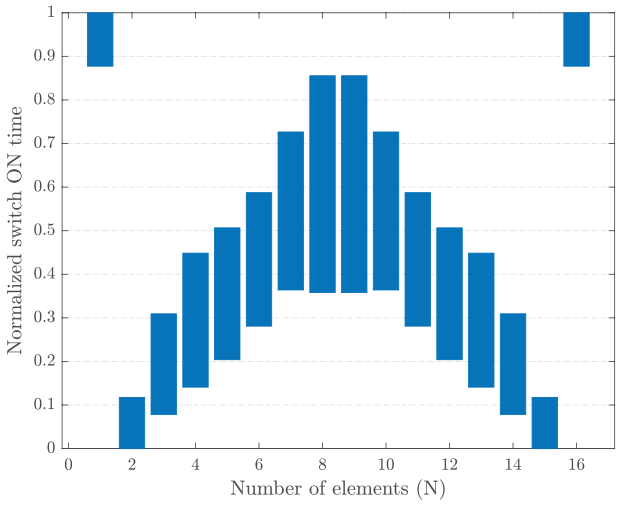

Figure 8. Switching sequence obtained with QNM-GA to generate the flat-top beam pattern in a 16-element TMLA for shaped pattern synthesis.

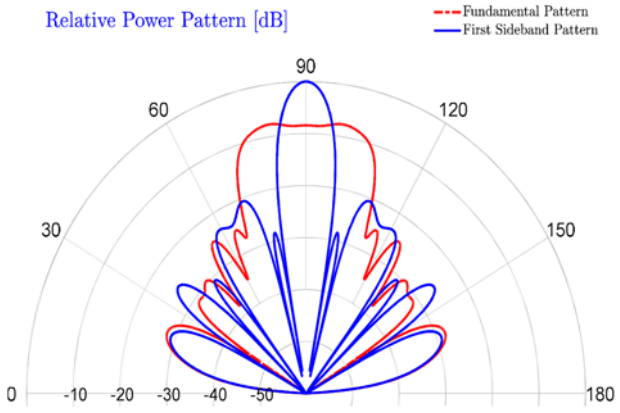

Figure 9. The corresponding shaped beam patterns at the first sideband ($m = 1$), obtained with the QNM-GA-based time scheme shown in Fig. 8.

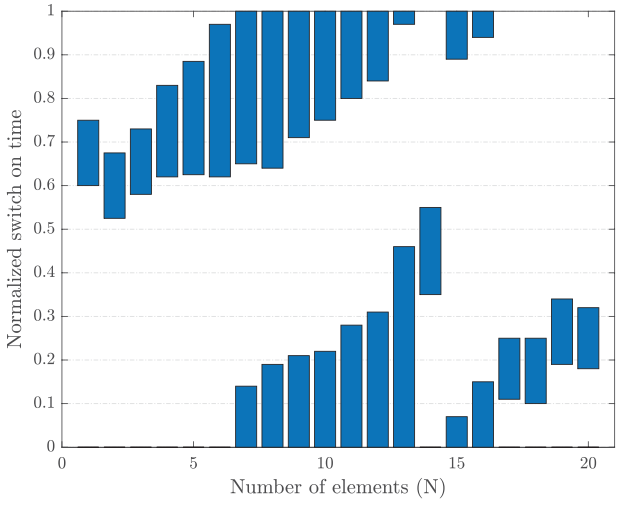

Figure 10. Switching sequence obtained with QNM-GA to generate the cosecant-squared beam pattern in a 20-element TMLA for cosecant pattern synthesis.

The optimized ON times and starting times are reported in Table 1. The results and the comparison with other published

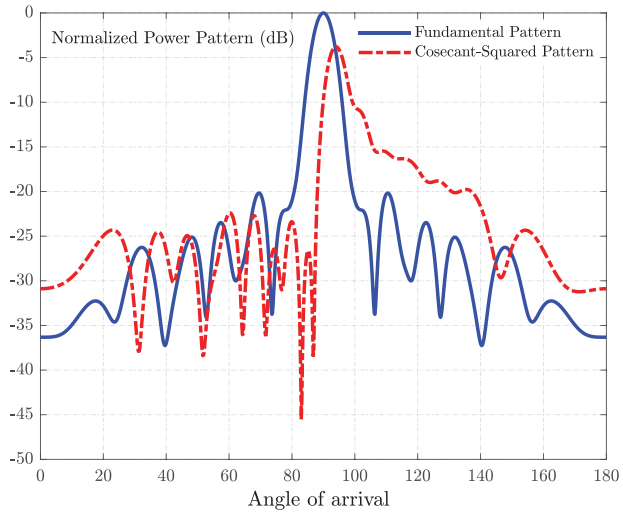

Figure 11. The corresponding cosecant-squared beam pattern at the first sideband ($m = 1$), obtained with the QNM-GA-based time scheme shown in Fig. 10.

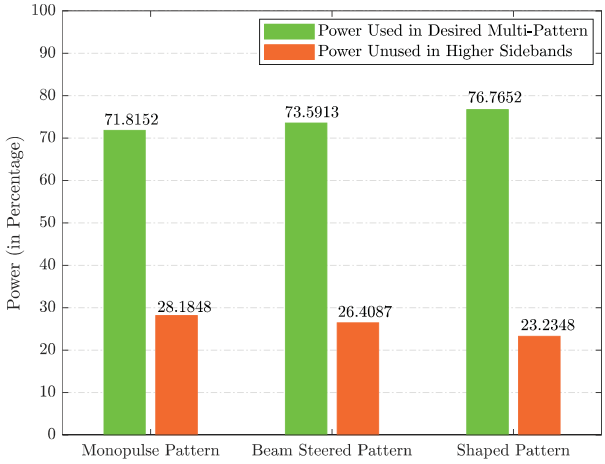

Figure 12. Dissipated power in proposed multi-beams and unused power in higher harmonics obtained with QNM-GA-based switching schemes.

results for the monopulse and scanned beam patterns are presented in Tables 2 and 3, respectively. The SLLs achieved for all the multi-patterns are relatively smaller than the other reported works. It is observed that the SLL_0 of monopulse and steered patterns are reduced to −40.89 dB and −33.12 dB compared to the best-reported results of −40 dB [9] and −21.7 dB [35], respectively. The proposed method also shows improvement in terms of SLL_1 as −22.54 dB and −23.58 dB is achieved compared to −20.1 dB [9] and −21.6 dB [35] of the best-reported works. From the comparison, it is clear that multiple patterns can be efficiently achieved with the proposed method. The total radiated power used by the synthesized multi-beams and the wasted power in other harmonic frequencies for all the proposed applications are presented in Fig. 12.

Conclusion

This work has proposed and verified an unorthodox but efficient substitute of traditional antenna arrays for multi-pattern synthesis. Multiple radiation patterns for monopulse and MFRs systems are investigated with fourth-dimensional (4D) antenna arrays, where

https://doi.org/10.1017/S1759078723000910 Published online by Cambridge University Press

the radiation patterns of the array are synthesized by controlling the ON times of each element. The monopulse scanning patterns are investigated by creating concurrent sum–difference beams with controlled radiating properties. The "fourth-dimensional" concept is further extended for MFRs where simultaneously scanned and shaped patterns are beneficial. Apart from the narrowband patterns for MFRs, the same concept is also exploited for wideband applications like shaped flat-top and cosecant-squared beam patterns. For all the desired beam patterns, utmost care has been taken to minimize the wanted inter-references. Furthermore, the higher-order harmonics inherently generated due to time-modulation are also suppressed to save power. All the examples are supported with simulated results and also compared with its counterpart results whenever applicable (and available) to show the enormous possibilities toward an alternate solution of phased antenna arrays. The "time-modulated" arrays can be implemented with high-speed switches eliminating costly phase shifters required in traditional phased arrays. The erroneous attenuators can also be discarded with uniform excitations. The dynamic range ratio obtained is 1, which is an added advantage of this work compared to traditional arrays. The SLLs of the monopulse beams are lowered below the ultra-low level (−40 dB). The SLLs of the scanned beams are also suppressed below −30 dB, whereas for wideband patterns, all the SLLs are suppressed below −20 dB. The power wasted in unwanted directions for all the patterns are also suppressed to improve the efficiencies. Thus, a cost-effective alternate to phased arrays for multi-pattern synthesis is proposed in this article, and the idea can be exploited further in near future.

Financial Support. This work is endorsed under the grant of EEQ/2021/000700 provided by SERB-DST.

Competing interest. The authors declare that they have no known competing financial interests or personal relationships that could have appeared to influence the work reported in this paper.

References

1. **Hansen RC** (2009) *Phased Array Antennas*, 2nd edn. Chang Kai Wiley Series in Microwave and Optical Engineering. Hoboken, New Jersey: John Wiley & Sons.
2. **Mailloux RJ** (2006) A history of phased array antennas. In *History of Wireless*, Chang, Kai Wiley Series in Microwave and Optical Engineering. Hoboken, New Jersey: John Wiley & Sons, 567–603.
3. **Chakraborty A, Ram G and Mandal D** (2021) Time-domain approach towards smart antenna design. In *Signals and Communication Technology*, Wideband, Multiband, and Smart Antenna Systems Switzerland AG: Springer, Cham, 363–394.
4. **Rocca P, Oliveri G, Mailloux RJ and Massa A** (2016) Unconventional phased array architectures and design methodologies—a review. *Proceedings of the IEEE* **104**(3), 544–560.
5. **Shanks HE and Bickmore RW** (1959) Four-dimensional electromagnetic radiators. *Canadian Journal of Physics* **37**, 263–275.
6. **Shanks HE** (1961) A new technique for electronic scanning. *IRE Transactions on Antennas and Propagation* **9**, 162–166.
7. **Kummer WH, Villeneuve AT, Fong TS and Terrio FG** (1963) Ultra-low sidelobes from time-modulated arrays. *IEEE Transactions on Antennas and Propagation* **11**, 633–639.
8. **Haupt RL** (2017) Antenna arrays in the time domain: An introduction to timed arrays. *IEEE Antennas and Propagation Magazine* **59**, 33–41.
9. **Yang S, Chen Y and Nie Z** (2008) Multiple patterns from time-modulated linear antenna arrays. *Electromagnetics* **28**, 562–571.
10. **Chakraborty A, Ram G and Mandal D** (2022) Electronic beam steering in timed antenna array by controlling the harmonic patterns with optimally derived pulse-shifted switching sequence. In *International Conference on Innovative Computing and Communications*, 205–216.
11. **Rocca P, Yang F, Poli L and Yang S** (2019) Time-modulated array antennas–theory, techniques, and applications. *Journal of Electromagnetic Waves and Applications* **33**(12), 1503–1531.
12. **Maneiro-Catoira R, Brégains J, García-Naya JA and Castedo L** (2017) Time modulated arrays: From their origin to their utilization in wireless communication systems. *Sensors* **17**(3), 590.
13. **Fondevila J, Brégains JC, Ares F and Moreno E** (2004) Optimizing uniformly excited linear arrays through time modulation. *IEEE Antennas and Wireless Propagation Letters* **3**, 298–301.
14. **Yang S, Gan YB and Tan PK** (2003) A new technique for power-pattern synthesis in time-modulated linear arrays. *IEEE Antennas and Wireless Propagation Letters* **2**, 285–287.
15. **Brégains JC, Fondevila-Gómez J, Franceschetti G and Ares F** (2008) Signal radiation and power losses of time-modulated arrays. *IEEE Transactions on Antennas and Propagation* **56**, 1799–1804.
16. **Yang S, Gan YB and Qing A** (2002) Sideband suppression in time-modulated linear arrays by the differential evolution algorithm. *IEEE Antennas and Wireless Propagation Letters* **1**, 173–175.
17. **Yang S, Can YB and Tan PK** (2004) Comparative study of low sidelobe time modulated linear arrays with different time schemes. *Journal of Electromagnetic Waves and Applications* **18**, 1443–1458.
18. **Tennant A and Chambers B** (2007) A two-element time-modulated array with direction-finding properties. *IEEE Antennas and Wireless Propagation Letters* **6**, 64–65.
19. **Li G, Yang S, Chen Y and Nie Z** (2009) A novel electronic beam steering technique in time modulated antenna arrays. *Progress in Electromagnetics Research* **97**, 391–405.
20. **Tong Y and Tennant A** (2010) Simultaneous control of sidelobe level and harmonic beam steering in time-modulated linear arrays. *Electronics Letters* **46**, 200–202.
21. **Poli L, Rocca P, Oliveri G and Massa A** (2011) Harmonic beamforming in time-modulated linear arrays. *IEEE Transactions on Antennas and Propagation* **59**, 2538–2545.
22. **Tong Y and Tennant A** (2012) A two-channel time modulated linear array with adaptive beamforming. *IEEE Transactions on Antennas and Propagation* **60**, 141–147.
23. **Poli L, Moriyama T and Rocca P** (2014) Pulse splitting for harmonic beamforming in time-modulated linear arrays. *International Journal of Antennas and Propagation* **2014**, 1–9.
24. **Chakraborty A, Mandal D and Ram G** (2019) Beam steering in a time switched antenna array with reduced side lobe level using evolutionary optimization technique. In *2019 IEEE Indian Conference on Antennas and Propagation, InCAP 2019*.
25. **Ram G, Panduro MA, Reyna A, Kar R and Mandal D** (2018) Pattern synthesis and broad nulling optimization of STMLAA with EM simulation. *International Journal of Numerical Modelling: Electronic Networks, Devices and Fields* **31**, e2322.
26. **Barton DK** (2010) History of monopulse radar in the US. *IEEE Aerospace and Electronic Systems Magazine* **25**, c1–c16.
27. **Sherman SM** (1985) Monopulse principles and techniques. *IEEE Antennas and Propagation Society Newsletter* **27**(5), 17.
28. **Chakraborty A, Ram G and Mandal D** (2021) Pattern synthesis of timed antenna array with the exploitation and suppression of harmonic radiation. *International Journal of Communication Systems* **34**, e4727.
29. **Chakraborty A, Ram G and Mandal D** (2021) Time-modulated multibeam steered antenna array synthesis with optimally designed switching sequence. *International Journal of Communication Systems* **34**, e4828.
30. **Chakraborty A, Ram G and Mandal D** (2021) Multibeam steered pattern synthesis in time-modulated antenna array with controlled harmonic radiation. *International Journal of RF and Microwave Computer-Aided Engineering* **31**, e22597.
31. **Chakraborty A, Ram G and Mandal D** (2020) Optimal pulse shifting in timed antenna array for simultaneous reduction of sidelobe and sideband level. *IEEE Access* **8**, 131063–131075.
32. **Chakraborty A, Ram G and Mandal D** (2022) Time-modulated linear array synthesis with optimal time schemes for the simultaneous

https://doi.org/10.1017/S1759078723000910 Published online by Cambridge University Press

suppression of sidelobe and sidebands. *International Journal of Microwave and Wireless Technologies* **14**, 768–780.
33. **Bhattacharya R, Saha S and Bhattacharyya TK** (2017) Mutated IWO optimized 4-D array for femtocell cognitive radio. *IEEE Antennas and Wireless Propagation Letters* **16**, 2614–2617.
34. **Chakraborty A, Ram G and Mandal D** (2019) Power pattern synthesis of a moving phase center time modulated antenna array using symmetrically and asymmetrically positioned time schemes. *International Journal of RF and Microwave Computer-Aided Engineering* **32**(12), e23442.
35. **Rocca P, Zhu Q, Bekele ET, Yang S and Massa A** (2014) 4-D arrays as enabling technology for cognitive radio systems. *IEEE Transactions on Antennas and Propagation* **62**, 1102–1116.
36. **Poddar S, Paul P, Chakraborty A, Ram G and Mandal D** (2022) Design optimization of linear arrays and time-modulated antenna arrays using meta-heuristics approach. *International Journal of Numerical Modelling: Electronic Networks, Devices and Fields* **35**(5), e3010.
37. **De Jong K, Fogel DB and Schwefel H-P** (2004) A history of evolutionary computation. In Baeck Thomas, Fogel DB and Michalewicz Z (eds.), *Handbook of Evolutionary Computation*, 1st edn. Oxford, United Kingdom: Oxford University Press, 988.
38. **Del Ser J, Osaba E, Molina D, Yang XS, Salcedo-Sanz S, Camacho D, Das S, Suganthan PN, Coello CA and Herrera F** (2019) Bio-inspired computation: Where we stand and what's next. *Swarm and Evolutionary Computation* **48**, 220–250.
39. **Ram G, Mandal D, Kar R and Ghoshal SP** (2014) Optimized hyper beamforming of receiving linear antenna arrays using Firefly algorithm. *International Journal of Microwave and Wireless Technologies* **6**, 181–194.
40. **Durmus A and Kurban R** (2021) Optimum design of linear and circular antenna arrays using equilibrium optimization algorithm. *International Journal of Microwave and Wireless Technologies* **13**, 986–997.
41. **Rattan M, Patterh MS and Sohi BS** (2009) Optimization of circular antenna arrays of isotropic radiators using simulated annealing. *International Journal of Microwave and Wireless Technologies* **1**, 441–446.
42. **Das A, Mandal D and Kar R** (2021) An optimal circular antenna array design considering the mutual coupling employing ant lion optimization. *International Journal of Microwave and Wireless Technologies* **13**, 164–172.
43. **Dib NI** (2015) Synthesis of thinned planar antenna arrays using teaching-learning-based optimization. *International Journal of Microwave and Wireless Technologies* **7**, 557–563.
44. **Bogdan G, Godziszewski K and Yashchyshyn Y** (2020) Experimental investigation of beam-steering applied to 2 × 2 MIMO system with single receiving RF chain and time-modulated antenna array. *International Journal of Microwave and Wireless Technologies* **12**, 504–512.
45. **Dib N and Sharaqa A** (2015) Design of non-uniform concentric circular antenna arrays with optimal sidelobe level reduction using biogeography-based optimization. *International Journal of Microwave and Wireless Technologies* **7**, 161–166.
46. **Ram G, Mandal D, Kar R and Ghoshal SP** (2017) Directivity improvement and optimal far field pattern of time modulated concentric circular antenna array using hybrid evolutionary algorithms. *International Journal of Microwave and Wireless Technologies* **9**, 177–190.
47. **Misra B and Mahanti GK** (2022) Meta-heuristic optimization algorithms for synthesis of reconfigurable hexagonal array antenna in two principle vertical planes. *International Journal of Microwave and Wireless Technologies* **14**, 158–165.
48. **Neri F and Cotta C** (2012) Memetic algorithms and memetic computing optimization: A literature review. *Swarm and Evolutionary Computation* **2**, 1–14.
49. **Weile DS and Michielssen E** (1997) Genetic algorithm optimization applied to electromagnetics: A review. *IEEE Transactions on Antennas and Propagation* **45**, 343–353.
50. **Zhang X, Lin M, Zhang X and Li Y** (2019) The design of microstrip array antenna and its optimization by a memetic method. *IEEE Access* **7**, 96434–96443.
51. **Li D, Qi L and Roshchina V** (2008) A new class of quasi-Newton updating formulas. *Optimization Methods & Software* **23**, 237–249.
52. **Zhou W and Zhang L** (2020) A modified Broyden-like quasi-Newton method for nonlinear equations. *Journal of Computational and Applied Mathematics* **372**, 112744.
53. **Fang X, Ni Q and Zeng M** (2018) A modified quasi-Newton method for nonlinear equations. *Journal of Computational and Applied Mathematics* **328**, 44–58.
54. **Krishna Chaitanya R, Raju GSN, Raju KVSN and Mallikarjuna Rao P** (2022) Antenna pattern synthesis using the quasi Newton method, firefly and particle swarm optimization techniques. *IETE Journal of Research* **68**(2), 1148–1156.
55. **Morabito AF, Di Carlo A, Di Donato L, Isernia T and Sorbello G** (2019) Extending spectral factorization to array pattern synthesis including sparseness, mutual coupling, and mounting-platform effects. *IEEE Transactions on Antennas and Propagation* **67**, 4548–4559.
56. **Palmeri R, Isernia T and Morabito AF** (2019) Diagnosis of planar arrays through phaseless measurements and sparsity promotion. *IEEE Antennas and Wireless Propagation Letters* **18**, 1273–1277.
57. **Ram G** (2021) Multi-beam steered harmonic pattern synthesis in timed antenna array with optimized and pre-defined RF switching. *International Journal of Numerical Modelling: Electronic Networks, Devices and Fields* **34**, e2912.

Avishek Chakraborty passed his B.Tech. degree in Electronics and Communication Engineering. He received his M.Tech. degree in Radio Physics and Electronics with a specialization in Space Science and Microwaves from the University of Calcutta, West Bengal, India, in 2017. He has completed his Ph.D. in Electronics and Communication Engineering from National Institute of Technology (NIT) Durgapur in 2021. He has also successfully completed a DST-SERB sponsored research project by serving as DST-SERB Research Fellow in his Ph.D. tenure. He is presently working as an Assistant Professor at the Department of Electrical, Electronics & Communication Engineering (EECE), GITAM University, Bangalore. He has authored several research papers published in peer-reviewed international journals, conferences, and book chapters. He has also served as a reviewer of *IEEE Access, International Journal of RF and Computer-Aided Engineering, Circuits Systems and Signal Processing, The Journal of Supercomputing*, etc. His current research interests include antenna array synthesis, phased arrays, antenna array optimization using soft computing and artificial intelligence, and signal processing for antenna arrays and radars.

Ravi Shankar Saxena received his B.E. degree in Electronics and Communication Engineering from Rohilkhand University, India, in 2000. He has completed his M.Tech. from MNNIT Allahabad in 2004, and D.Phil. in Communication Technology from Department of Electronics and Communication, University of Allahabad in 2016. He has published more than 16 research papers in different national and international journals and conference proceedings. His areas of interests include Patch antenna, Experimental nanoscience including Nanostructure fabrication, Optoelectronics properties, and Energy technologies. He is currently working as a Professor in GMRIT, Razam, Andhra Pradesh, India.

https://doi.org/10.1017/S1759078723000910 Published online by Cambridge University Press

Anshoo Verma is working as Assistant Professor in Department of Civil Engineering, IES Institute of Technology and Management at IES University, Bhopal, since last 3 years. He has experience of more than 3 years in academics and research. Dr. Verma has completed his Master of Technology in Construction Technology and Management from Oriental Institute of Science & Technology in 2021.

Ashima Juyal has been working in the Department of Electronics & Communication Engineering at Uttaranchal Institute of Technology, Uttaranchal University, Dehradun, India. She has experience of more than 5 years in research and academics. Ms. Ashima is currently deputed at Research and Innovations Division at Uttaranchal University. Her areas of interests are Internet of Things, fuzzy logics, blockchain, and deep learning.

Sumit Gupta is working as Assistant Professor in the Department of Electronics and Communication at SR University, boasts over 13 years of experience in the field of educational profession and research, having previously served as a faculty member at KL University. He completed Ph.D. in Optical Multiplexing Technique in Fiber Communication from the prestigious National Institute of Technology, Bhopal, completed in 2017. He published his work in various reputed journals. Dr. Gupta currently focuses his research efforts on the cutting-edge fields of quantum communication and free space optical technology, exploring advanced multiplexing techniques.

Indrasen Singh is working as an Assistant Professor in the School of Electronics Engineering, VIT Vellore, Tamil Nadu, India. He received his B.Tech. and M.Tech. Degrees in electronics and communication engineering from Uttar Pradesh Technical University, Lucknow, India, in 2006, and 2010, respectively. He obtained his Ph.D. degree in electronics and communication engineering from National Institute of Technology Kurukshetra, Haryana, India, in 2019. He has more than 12 years of teaching, research experience in various reputed technical institutes or universities. He is the editorial board member of AJECE, Science Publishing Group, USA. He is the reviewer of many international journals and served as TPC member and reviewer in different conferences. He has published more than 20 research papers in national/international journals/conferences of repute and many are under review. His research interests are in the area of cooperative communication, stochastic geometry, modeling of wireless, heterogeneous networks, millimeter wave communications, device-to-device, and 5G/6G communication.

Gopi Ram completed his B.E. degree in Electronics and Telecommunication Engineering from Government Engineering College, Jagdalpur, Chhattisgarh, India, in the year 2007. He received his M.Tech. degree in Telecommunication Engineering from National Institute of Technology Durgapur, West Bengal, India, in the year 2011. He joined as a full-time Institute Research Scholar in the year of 2012 at National Institute of Technology, Durgapur, to carry out research for Ph.D. degree. He received the scholarship from the Ministry of Human Resource and Development (MHRD), Government of India, for the period 2009–2011 (M. Tech) and 2012–2015 (Ph.D). He is currently working as an Assistant Professor at the Department of Electronics and Communication Engineering, National Institute of Technology, Warangal, Telangana, India. His research interests include evolutionary optimization-based radiation pattern synthesis of antenna arrays, time-modulated antenna arrays, and applications of soft computing techniques in electromagnetics. He has published more than 50 research papers in international journals and conferences.

Durbadal Mandal completed his B.E. degree in Electronics and Communication Engineering from Regional Engineering College, Durgapur, West Bengal, India, in the year 1996. He received M.Tech. and Ph.D. degrees from National Institute of Technology, Durgapur, West Bengal, India, in the year 2008 and 2011, respectively. Presently, he is attached with National Institute of Technology Durgapur, West Bengal, India, as Associate Professor in the Department of Electronics and Communication Engineering. He has supervised 16 doctoral students and has completed 2 DST-SERB Sponsored Research Projects as Project Investigator till date. His research interest includes array antenna design; filter optimization via evolutionary computing techniques. He has published more than 350 research papers in international journals and conferences.

https://doi.org/10.1017/S1759078723000910 Published online by Cambridge University Press